Computers & Fluids 108 (2015) 1–12

Contents lists available at ScienceDirect

Computers & Fluids

journal homepage: www.elsevier.com/locate/compfluid

# A numerical study of the effect of particle properties on the radial distribution of suspensions in pipe flow

Arman Pazouki, Dan Negrut *

*Department of Mechanical Engineering, University of Wisconsin–Madison, Madison, WI 53706-1572, USA*

ARTICLE INFO

*Article history:*
Received 23 July 2014
Received in revised form 10 November 2014
Accepted 22 November 2014
Available online 28 November 2014

*Keywords:*
Pipe flow
Particle radial migration
Direct numerical simulation
Fluid–solid interaction
Lagrangian–Lagrangian approach
Smoothed Particle Hydrodynamics

ABSTRACT

We employ a Lagrangian–Lagrangian (LL) numerical formalism to study two- and three-dimensional (2D, 3D) pipe flow of dilute suspensions of macroscopic neutrally buoyant rigid bodies at flow regimes with Reynolds numbers (Re) between 0.1 and 1400. A validation study of particle migration over a wide spectrum of Re and average volumetric concentrations demonstrates the good predictive attributes of the LL approach adopted herein. Using a scalable parallel implementation of the approach, 3D direct numerical simulation is used to show that (1) rigid body rotation affects the behavior of a particle laden flow; (2) an increase in neutrally buoyant particle size decreases radial migration; (3) a decrease in inter-particle distance slows down the migration and shifts the stable position further away from the channel axis; (4) rigid body shape influences the stable radial distribution of particles; (5) particle migration is influenced, both quantitatively and qualitatively, by the Reynolds number; and (6) the stable radial particle concentration distribution is affected by the initial concentration. The parallel LL simulation framework developed herein does not impose restrictions on the shape or size of the rigid bodies and was used to simulate 3D flows of dense, colloidal suspensions of up to 23,000 neutrally buoyant ellipsoids.



## 1. Introduction

The topic of particle migration has been of great interest since Segre and Silberberg experimentally investigated the pipe flow of a dilute suspension of spherical particles and demonstrated that, at a pipe Reynolds number (*Re*) between 2 and 700, the particles settle on an annulus with an approximate relative radius of 0.6 with respect to the pipe radius [64,65]. Subsequent experiments conducted by Oliver [53], Jeffrey and Pearson [32], and Karnis et al. [34] confirmed and further investigated the particle radial migration. For dilute suspensions, Matas et al. [42] showed experimentally that the radius of stable annulus increases directly with *Re*. At a high Reynolds number, $Re > 650$, they observed the formation of an inner annulus of smaller radius that had not been predicted analytically or observed through simulation. Moreover, they showed that the probability of a particle settling on this annulus of smaller radius increases with the Reynolds number. From an analytical perspective, perturbation methods have been widely employed to investigate the lift force responsible for particle migration, see for instance Saffman [61], Ho and Leal [26], Vasseur and Cox [71], Schonberg and Hinch [63], Hogg [28], Asmolov et al. [2], and Matas et al. [43]. Particle migration has also been investigated in a number of numerical simulation studies. Feng et al. [19] employed a Finite Element Method (FEM) to study the migration of a single circular cylinder in plane Poiseuille flow. Inamuro et al. [31] investigated a similar problem using a Lattice Boltzmann Method (LBM). Chun and Ladd employed LBM to investigate the migration of spheres in a square duct at $Re < 1000$ [11]. They showed that the stable lateral position of a single particle moves closer to the duct wall as the Reynolds number increases. For flows containing several particles, a first stable particle configuration forms at $Re < 300$; a secondary stable region nearer to the center of the duct is observed at $Re > 700$. Pan and Glowinski developed the method of Distributed Lagrange Multiplier/Fictitious Domain Method (DLM/FDM) in conjunction with a finite difference approach to investigate the shear induced migration of a circular cylinder [22] and a collection of spheres [57]. Shao et al. [66] investigated the motion of spheres in steady Poiseuille flow at moderately high *Re* using DLM/FDM. Their work confirmed the development of an inner stable annulus at high *Re*, i.e., $Re \geqslant 640$ for specific size and channel length ratio. Yu et al. [73] investigated the sphere sedimentation as well as the migration of a sphere in Poiseuille flow at $Re < 400$ via the DLM method. Hu [30] and Hu et al. [29] employed the Arbitrary Lagrangian–Eulerian (ALE) method on a body-fitted unstructured finite element grid to simulate fluid–solid systems. Their work influenced that of Patankar et al. [59,58] and Choi and Josef [9] in their study of the lift-off of

* Corresponding author.
*E-mail addresses:* pazouki@wisc.edu (A. Pazouki), negrut@wisc.edu (D. Negrut).

http://dx.doi.org/10.1016/j.compfluid.2014.11.027
0045-7930/

cylinders in plane Poiseuille flow. Similar techniques have been considered to study the behavior of a non-spherical particle, usually an ellipsoid in fluid flow. Swaminathan et al. [69] used ALE based FEM to simulate the sedimentation of an ellipsoid. Pan et al. [54] investigated the motion of ellipsoid in Poiseuille flow using DLM/FDM. In several other studies the investigation of flows containing a collection of cylinders (2D) [8,20,67] and spheres (3D) [11,29] was carried out via direct numerical simulation with the LBM [11,20], Lagrange multiplier based fictitious domain method [8,56,67], and ALE-based FEM [29].

All these numerical studies of particle suspension and migration draw on an Eulerian–Lagrangian representation of the fluid–solid system. In this contribution, we employ a Lagrangian–Lagrangian (LL) approach to study the particle migration over a wide range of Reynolds numbers. The Smoothed Particle Hydrodynamics (SPH) method [21,41] is relied upon for the fluid flow simulation. The SPH method is extensively reviewed in Monaghan [47] and Liu and Liu [40]. Herein, the Navier–Stokes equations, solved within the SPH framework, are coupled with Newton's equations of motion for rigid body dynamics to investigate, in a unitary framework, flows that include rigid bodies of arbitrary geometries. We used and validated the coupling algorithm reported in [60]. The possible solid to solid contacts, if any, are resolved via a lubrication force model [39].

The document is organized as follows: Section 2 provides an overview of the numerical solution and its parallel implementation. Section 3 presents a set of validations of the proposed approach in relation to experiments that involve particle migration and distribution at $1 < Re < 1400$. The distribution validation exhibits more complexity than capturing only the stable radial position since attention must be paid to the rate of migration to the stable configuration. In Section 4, we report results of several parametric studies that investigate the effect of particle shape, size, distance, and concentration on particle radial migration. A scaling analysis carried out for a dense colloidal suspension of ellipsoids concludes the numerical experiment section.

## 2. Fluid–solid interaction simulation methodology

The SPH-based approach used herein to represent the dynamics of fluid flow accounts for the two-way coupling with rigid body dynamics by regarding body geometries as moving boundaries. The 3D rigid body rotation is characterized by means of a set of four Euler parameters [25]. In terms of notation, the term "marker" is employed to denote the SPH discretization point and "particle" to refer to a 3D rigid body, although the latter has geometry and experiences 3D rotation during its time evolution.

### 2.1. The Smoothed Particle Hydrodynamics method

An in-depth discussion of the SPH method and recent developments can be found in [40,44,47]. Herein, we highlight the essential components required to express the fluid–solid coupling.

SPH is a Lagrangian method that probes the fluid domain at a set of moving markers. Each marker has an associated kernel function with compact support that defines its domain of influence, as shown in Fig. 1. The choice of kernel function $W$ is not unique. A cubic spline interpolation kernel [48] was used in this work. At a point located by a position vector $\mathbf{r}$ with respect to an SPH marker, the cubic spline interpolation kernel is defined as

$$W(q,h) = \frac{1}{4\pi h^3} \times \begin{cases} (2-q)^3 - 4(1-q)^3, & 0 \leqslant q < 1 \\ (2-q)^3, & 1 \leqslant q < 2 \\ 0, & q \geqslant 2 \end{cases}, \tag{1}$$

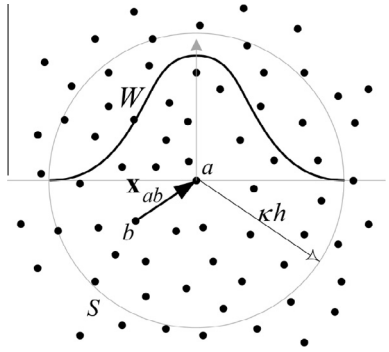


**Fig. 1.** Illustration of the kernel, $W$, and support domain, S – shown for marker a. For 2D problems the support domain is a circle, while for 3D problems it is a sphere. SPH markers are shown as black dots.

where $h$ is the kernel function's characteristic length and $q \equiv |\mathbf{r}|/h$. The radius of the support domain, $\kappa h$, is proportional to the characteristic length $h$ through the parameter $\kappa$ which is equal to 2 in the kernel function defined by Eq. (1). Although, a constant $h$ was considered herein, using a variable $h$ may be beneficial in some applications such as wave propagation in compressible flow [47].

The cubic spline kernel given in Eq. (1) is the most common smoothing kernel in one, two, and three dimensions owing to its reduced computational burden – a consequence of the small number of neighboring SPH markers typically required by the approach. Other researchers suggested that a smoother second order derivative of the interpolation kernel can improve the SPH stability [40,51,70]. In [50] it was shown that the dispersion relation for linear waves can be undesirable for cubic splines with $\kappa = 2$. However, depending on the application, the artifacts can be negligible. Kernels that approximate the Gaussian function; i.e., higher order splines such as quartic ($\kappa = 2.5$) and quintic ($\kappa = 3$), have been shown to produce better results at the expense of a higher computational burden [51]. Similarly, Colagrossi and Landrini [12] tested third and fifth order B-splines as well as cut-normalized Gaussian kernels ($\kappa = 3$), and recommended the latter.

Using the SPH framework, the continuity and momentum equations, given respectively by

$$\frac{d\rho}{dt} = -\rho \nabla \cdot \mathbf{v}, \tag{2}$$

and

$$\frac{d\mathbf{v}}{dt} = -\frac{1}{\rho}\nabla p + \frac{\mu}{\rho}\nabla^2 \mathbf{v} + \mathbf{f}, \tag{3}$$

are discretized as [49]

$$\frac{d\rho_a}{dt} = \rho_a \sum_b \frac{m_b}{\rho_b}(\mathbf{v}_a - \mathbf{v}_b) \cdot \nabla_a W_{ab}, \tag{4}$$

and

$$\frac{d\mathbf{v}_a}{dt} = -\sum_b m_b \left( \left( \frac{p_a}{\rho_a^2} + \frac{p_b}{\rho_b^2} \right) \nabla_a W_{ab} + \Pi_{ab} \right) + \mathbf{f}_a. \tag{5}$$

In Eq. (5), indices $a$ and $b$ denote the SPH markers, as shown in Fig. 1, and

$$\Pi_{ab} = -\frac{(\mu_a + \mu_b)\mathbf{x}_{ab} \cdot \nabla_a W_{ab}}{\bar{\rho}_{ab}^2 (x_{ab}^2 + \varepsilon \bar{h}_{ab}^2)} \mathbf{v}_{ab} \tag{6}$$

imposes the viscous force based on the discretization of the $\nabla^2$ operator. In terms of notation, $\rho$ and $\mu$ are the fluid density and viscosity, respectively; $\mathbf{v}$ and $p$ are flow velocity and pressure, respectively; $m$ is the mass associated with an SPH marker; $\mathbf{f}$ is the volumetric force; $t$ is the real time; $\mathbf{x}_{ab}$ is the relative distance